

Properties of light (anti)nuclei and (anti) hypertriton production in Pb-Pb collisions at $\sqrt{s_{NN}} = 2.76$ TeV

Zhilei She¹, Gang Chen^{1,2*}, Hongge Xu¹, Tingting Zeng¹, Dikai Li¹

¹*School of Mathematics and Physics, China University of Geosciences, Wuhan 430074, China.*

²*Key Laboratory of Quark and Lepton Physics (MOE),
Central China Normal University, Wuhan 430079, China*

We investigate the properties of light (anti)nuclei and (anti)hypertriton production in Pb-Pb collisions at $\sqrt{s_{NN}} = 2.76$ TeV, based on the parton and hadron cascade and dynamically constrained phase-space coalescence (PACIAE+DCPC) model. We found that the yields of light (anti)nuclei and (anti)hypertriton strongly depend on the centrality, i.e., their yields decrease rapidly with the increase of centrality bins; but their yield ratios are independent of centrality. The results of our theoretical model are well consistent with ALICE data. Furthermore, we found that the integrated yields of (anti)nuclei per participant nucleon increase from peripheral to central collisions and more rapidly with increasing mass number. The transverse momentum distributions of the \bar{d} , d , $\frac{3}{\Lambda}\bar{H}$, $\frac{3}{\Lambda}H$, $\bar{3}He$ and $3He$ are also discussed in the 0-10% most central Pb-Pb collisions. The coalescence parameters B_A of light (anti)nuclei and (anti)hypernuclei are analyzed.

I. INTRODUCTION

Antimatter production has received considerable attention in particle and nuclear physics, astrophysics, cosmology and other fields of modern physics, since Dirac predicted the existence of negative energy states (i.e., antimatter) of electrons in 1928. The antiprotons [1] were discovered in 1955, and antineutrons [2] were discovered in 1956, followed by a series of antimatter nuclei including anti-deuterons, anti-triton, the anti-helium-3 in scientific experiments [3–6]. The hot and dense matter forms in ultra-relativistic heavy-ion collisions, which contains roughly equal numbers of quarks and anti-quarks [7], is similar to the fireball environment in the initial stages of the Big Bang. Thus, the ultra-relativistic heavy-ion collisions provide a good experimental condition [8] to study the production of light (anti)nuclei and the evolution of the early universe.

In 1995, the first production of anti-hydrogen atoms was detected [9], and then which was trapped successfully with a confinement time of 172 ms by the ALPHA [10] at the European Organization for Nuclear Research (CERN). Moreover, the ALICE Collaboration has also published its preliminary \bar{d} yield of $\sim 6 \times 10^{-5}$ measured in the proton-proton collisions at $\sqrt{s} = 7$ TeV [11]. At BNL (the Brookhaven National Laboratory), the STAR Collaboration has reported their measurements of $\frac{3}{\Lambda}\bar{H}$ [12] and $\bar{4}He$ [8] in Au-Au collisions at the top RHIC energy, respectively.

In theory, firstly the nucleons and hyperons are usually calculated with some selected models, such as the transport model. Then, the light nuclei (anti-nuclei) are studied by the reasonable hadron final-state coalescence models [13–17], such as the phase-space coalescence model [18–20] and/or the statistical model [21, 22],

etc. For example, the production of light nuclei (hyper-nuclei) in the Au-Au and Pb-Pb collisions at relativistic energies was described theoretically by the coalescence + blast-wave method [23] and the UrQMD-hydro hybrid model + thermal model [24], respectively.

Recently, we have proposed an approach studying the light nuclei (anti-nuclei) production in the relativistic heavy ion collisions by the dynamically constrained phase-space coalescence model (DCPC) [25], which is based on the final state hadronic generated by a parton and hadron cascade model PACIAE [26]. Using this method, the light nuclei (anti-nuclei) yields, transverse momentum distribution, and rapidity distribution in non-single diffractive proton-proton collisions at $\sqrt{s} = 7$ TeV [25] are predicted. The light nuclei (anti-nuclei) and hypernuclei (anti-hypernuclei) productions [27], their centrality dependence [28] and their mass number scaling property [29] in the Au-Au collisions at $\sqrt{s_{NN}} = 200$ GeV are also investigated. Moreover, The energy dependence of the ratio for antiparticle to particle is studied in the high energy proton-proton collisions [30]. In this paper, we will use this method to investigate the light nuclei (anti-nuclei) and hypernuclei (anti-hypernuclei) productions and the properties in the Pb-Pb collisions at $\sqrt{s_{NN}} = 2.76$ TeV.

The paper is organized as follows: In Sec. II, we briefly introduce the PACIAE and DCPC model. In Sec. III, our calculated results of light nuclei (anti-nuclei) and hypertriton (anti-hypertriton) are presented, such as their yields, ratios, the transverse momentum distributions, and are compared with the ALICE data. In Sec. IV, a short summary is given.

II. MODELS

The PACIAE model [26] is based on PYTHIA6.4 [31] and is designed mainly for nucleus-nucleus collisions. In the PACIAE model, the process is decomposed into four

*Corresponding Author: chengang1@cug.edu.cn

steps. Firstly, the nucleus-nucleus collision is decomposed into the nucleon-nucleon(NN) collisions according to the collision geometry and NN total cross section. Each NN collision is described by the PYTHIA model with the string fragmentation switches off and the di-quarks (antidiquarks) randomly breaks into quarks(anti-quarks). So the consequence of a NN collision is a partonic initial state composed of quarks, anti-quarks, and gluons. Provided all NN collisions are exhausted, one obtains a partonic initial state for a nucleus-nucleus collision. This partonic initial state is regarded as the quark-gluon matter(QGM) formed in relativistic nucleus-nucleus collisions. Secondly, the parton rescattering proceeds. The rescattering among partons in QGM is randomly considered by the $2 \rightarrow 2$ LO-pQCD parton-parton cross sections [32]. In addition, a K factor is introduced here to account for higher order and non-perturbative corrections. Thirdly, hadronization happens after parton rescattering. The partonic matter can be hadronized by the Lund string fragmentation regime [31] and/or the phenomenological coalescence model [26]. Finally, the hadronic matter continues rescattering until the hadronic freeze-out (the exhaustion of the hadron-hadron collision pairs). We refer to [26] for the details.

With the final state particles provided by the PACIAE model, we can then calculate the production of light nuclei (anti-nuclei) with the DCPC model. In quantum statistical mechanics [33], one cannot precisely define both position $\vec{q} \equiv (x, y, z)$ and momentum $\vec{p} \equiv (p_x, p_y, p_z)$ of a particle in the six-dimension phase space because of the uncertainty principle $\Delta\vec{q}\Delta\vec{p} \geq h^3$. We can only say that this particle lies somewhere within a six-dimension quantum box or state with a volume of $\Delta\vec{q}\Delta\vec{p}$. A particle state occupies a volume of h^3 in the six-dimension phase space [33]. Therefore, one can estimate the yield of a single particle by defining an integral $Y_1 = \int_{H \leq E} \frac{d\vec{q}d\vec{p}}{h^3}$, where H and E are the Hamiltonian and energy of the particle, respectively. Similarly, the yield of the N particle cluster can be estimated as the following integral:

$$Y_N = \int \dots \int_{H \leq E} \frac{d\vec{q}_1 d\vec{p}_1 \dots d\vec{q}_N d\vec{p}_N}{h^{3N}}. \quad (1)$$

In addition, equation (1) must satisfy the following constraint conditions:

$$m_0 \leq m_{inv} \leq m_0 + \Delta m, \quad (2)$$

$$q_{ij} \leq D_0, (i \neq j; i, j = 1, 2, \dots, N). \quad (3)$$

where

$$m_{inv} = \left[\left(\sum_{i=1}^N E_i \right)^2 - \left(\sum_{i=1}^N \vec{p}_i \right)^2 \right]^{1/2}, \quad (4)$$

and $E_i, \vec{p}_i (i=1, 2, \dots, N)$ are the energies and momenta of particles, respectively. m_0 and D_0 stand for, respectively,

the rest mass and diameter of light (anti)nuclei, Δm refers to the allowed mass uncertainty, and $q_{ij} = |\vec{q}_i - \vec{q}_j|$ is the vector distance between particles i and j . Because the hadron position and momentum distributions from transport model simulations are discrete, the integral over continuous distributions in equation (1) should be replaced by the sum over discrete distributions.

III. RESULTS AND DISCUSSION

First we produce the final state particles using the PACIAE model [26]. In the PYTHIA simulations, we assume that hyperons heavier than Λ decayed already. The model parameters are fixed on the default values given in PYTHIA [31]. However, the K factor as well as the parameters $\text{parj}(1)$, $\text{parj}(2)$, and $\text{parj}(3)$, which are relevant to the hadrons production in PYTHIA, are given by fitting the ALICE data of p, \bar{p}, Λ in Pb-Pb collisions at $\sqrt{s_{NN}} = 2.76$ [34, 35]. Specific details of this method is similar to the paper [28]. The fitted parameters of $K = 3$ (default value is 1 or 1.5 [31]), $\text{parj}(1) = 0.15(0.1)$, $\text{parj}(2) = 0.38(0.3)$, and $\text{parj}(3) = 0.65(0.4)$ are used to generate 1.833×10^6 minimum-bias events by the PACIAE model for the 0-20% centrality Pb-Pb collisions at $\sqrt{s_{NN}} = 2.76$ TeV with $|y| < 0.5$ acceptances, as shown in Table I.

TABLE I: The integrated yield dN/dy of particles at midrapidity ($|y| < 0.5$), for p, \bar{p} and Λ in Pb-Pb collisions of $\sqrt{s_{NN}} = 2.76$ TeV with 0-20% centrality.

Particle type	ALICE ^a	PACIAE
p	25.9 ± 1.6	25.9
\bar{p}	26.0 ± 1.8	24.8
Λ	19.3 ± 1.4	19.18

^a The ALICE data are taken from Ref. [34, 35].

Then, the integrated yields dN/dy of light (anti)nuclei d (\bar{d}), ${}^3\text{He}$ (${}^3\bar{\text{He}}$), as well as ${}^3_\Lambda\text{H}$ (${}^3_\Lambda\bar{\text{H}}$) are calculated by the DCPC model for each centrality bin of 0-5%, 5-10%, 10-20%, 20-30%, 30-50% as well as 50-80%, as shown in Tab. II. One can see from Table II that the yields dN/dy of light (anti)nuclei and (anti)hypertritons calculated by the DCPC model decrease (or increase) with the increase of centrality (or N_{part}); the yields of (anti)nuclei decrease with the increase of mass; and the yields of anti-nuclei are less than that of its corresponding nuclei.

In order to facilitate comparison with the experimental data, the cumulate yield Y_c is described as

$$Y_c = \frac{1}{C} \int_0^C \frac{dN}{dy} dc. \quad (5)$$

Where c is the value of centrality bins. The Fig. 1 effectively shows the cumulative yields Y_c of $d, \bar{d}, {}^3_\Lambda\text{H}, {}^3_\Lambda\bar{\text{H}}$,

TABLE II: The integrated yields dN/dy of d , \bar{d} , ${}^3\text{He}$, $\overline{{}^3\text{He}}$, ${}^3_\Lambda\text{H}$ and $\overline{{}^3_\Lambda\text{H}}$ calculated by PACIAE+DCPC model in midrapidity Pb-Pb collisions of $\sqrt{s_{\text{NN}}} = 2.76$ TeV. $\langle N_{\text{part}} \rangle$ is shown for each centrality bin.

Centrality	0% – 5%	5% – 10%	10% – 20%	20% – 30%	30% – 50%	50% – 80%
$\langle N_{\text{part}} \rangle$	379	323	256	186	110	36
d^a	0.112	0.0917	0.0703	0.0461	0.0199	0.00345
\bar{d}^a	0.101	0.0838	0.0631	0.0412	0.0182	0.00311
${}^3\text{He}^b$	3.84E-04	2.95E-04	2.13E-04	1.12E-04	4.99E-05	5.13E-06
$\overline{{}^3\text{He}}^b$	3.29E-04	2.51E-04	1.82E-04	9.44E-05	4.30E-05	4.29E-06
${}^3_\Lambda\text{H}^c$	4.47E-05	3.40E-05	2.33E-05	1.16E-05	5.94E-06	5.67E-07
$\overline{{}^3_\Lambda\text{H}}^c$	3.24E-05	2.45E-05	1.71E-05	8.26E-06	4.38E-06	4.03E-07

^a calculated with $\Delta m = 0.00042$ GeV for d , \bar{d} .

^b calculated with $\Delta m = 0.00091$ GeV for ${}^3\text{He}$, $\overline{{}^3\text{He}}$.

^c calculated with $\Delta m = 0.00040$ GeV for ${}^3_\Lambda\text{H}$, $\overline{{}^3_\Lambda\text{H}}$.

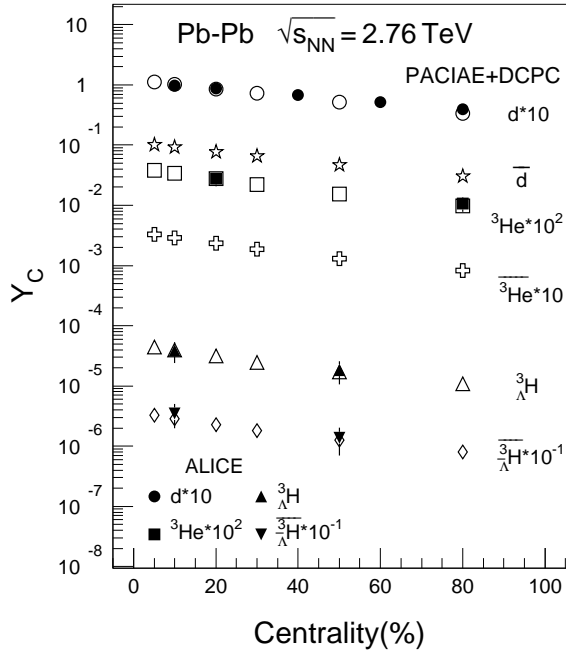


FIG. 1: The cumulative yields Y_C for light (anti)nuclei and (anti)hyper-triton as a function of centrality in midrapidity Pb-Pb collisions at $\sqrt{s_{\text{NN}}} = 2.76$ TeV. The solid symbols are the experimental data points from ALICE [36, 37]. The open symbols represent the outcome for our PACIAE+DCPC model.

${}^3\text{He}$ and $\overline{{}^3\text{He}}$ in different centrality bins Pb-Pb collisions at $\sqrt{s_{\text{NN}}} = 2.76$ TeV. One can see in Fig. 1, as well as Tab. II, the yields of light (anti)nuclei and (anti)hyper-triton all decrease rapidly with the increase of centrality, presenting a fall as the index distribution. Meanwhile, the PACIAE+DCPC model results (the open symbols) are consistent with the ALICE experimental data [36, 37]

(the solid symbols).

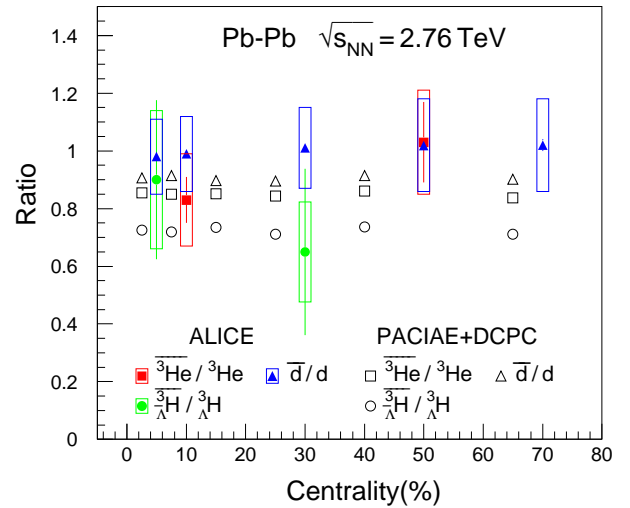


FIG. 2: Yield ratios of light anti-nuclei and anti-hypertriton (\bar{d} , $\overline{{}^3\text{He}}$, and $\overline{{}^3_\Lambda\text{H}}$) to light nuclei and hyper-triton (d , ${}^3\text{He}$, and ${}^3_\Lambda\text{H}$) in midrapidity Pb-Pb collisions at $\sqrt{s_{\text{NN}}} = 2.76$ TeV, plotted as a function of centrality. Open symbols represent our PACIAE+DCPC model results. Solid symbols are the experimental data points from ALICE [36, 37], which statistical uncertainties are represented by bars and systematic uncertainties are represented by open boxes.

In Fig. 2, the yield ratios of light anti-nuclei and anti-hypertriton (\bar{d} , $\overline{{}^3\text{He}}$, and $\overline{{}^3_\Lambda\text{H}}$) to light nuclei and hyper-triton (d , ${}^3\text{He}$ and ${}^3_\Lambda\text{H}$), are given in different centrality Pb-Pb collisions at $\sqrt{s_{\text{NN}}} = 2.76$ TeV. To facilitate comparison, experimental results from ALICE [36, 37] are also given with the solid points. One can see from Fig. 2, the yield ratios of light anti-nuclei to light nuclei and anti-hypertriton to hyper-triton from central to peripheral collisions remain unchanged, and their cor-

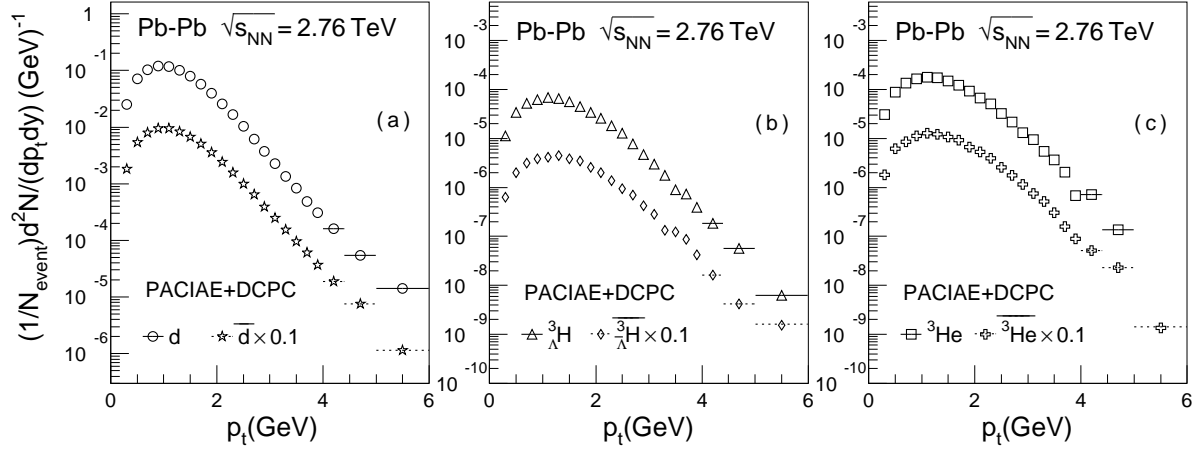


FIG. 3: The results (open points) of the transverse momentum distributions of light anti(nuclei) for PACIAE+DCPC model in the 0-10% most central Pb-Pb collisions at $\sqrt{s_{NN}} = 2.76$ TeV with $|y| < 0.5$ acceptances, calculated for (a) d and \bar{d} , (b) $\frac{3}{\Lambda}H$ and $\frac{3}{\Lambda}\bar{H}$, and (c) ${}^3\bar{He}$ and 3He .

responding values are respectively about 0.91, 0.85, 0.72, although their yields decrease rapidly with the centrality as shown in Tab. II and Fig. 1. The results obtained from our model are also in agreement with the experimental data from ALICE [36, 37] within error ranges.

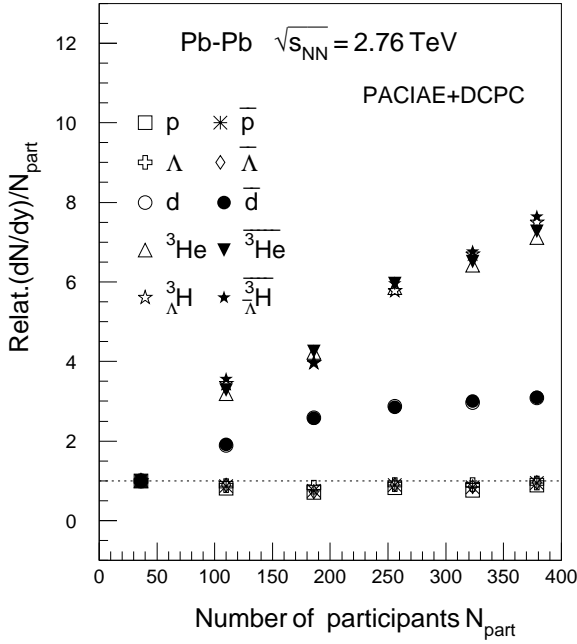


FIG. 4: The integrated yield dN/dy as a function of N_{part} . The yields at midrapidity for $p, \bar{p}, \Lambda, \bar{\Lambda}, d, \bar{d}, \frac{3}{\Lambda}H, \frac{3}{\Lambda}\bar{H}, {}^3He, {}^3\bar{He}$ are divided by N_{part} , normalized to the peripheral collisions (50%-80%). The results are calculated by PACIAE+DCPC model in Pb-Pb collisions at $\sqrt{s_{NN}} = 2.76$ TeV.

In Fig. 3, the transverse momentum distributions of $d, \bar{d}, \frac{3}{\Lambda}H, \frac{3}{\Lambda}\bar{H}, {}^3He$ and ${}^3\bar{He}$ calculated were shown in the

0-10% central Pb-Pb collisions at $\sqrt{s_{NN}} = 2.76$ TeV with $|y| < 0.5$ acceptances. Figures 3(a), 3(b) and 3(c) are the calculated the transverse momentum p_t distributions for $d(\bar{d}), \frac{3}{\Lambda}H(\frac{3}{\Lambda}\bar{H})$, as well as ${}^3He({}^3\bar{He})$, respectively. The pattern of light (anti)nuclei transverse momentum distributions is similar to the ALICE [11, 37] of transverse momentum. In addition, you can see that the the peak of transverse distribution appears at similar range for nuclei and anti-nuclei situations.

TABLE III: The results of the light (anti)nuclei average transverse momentum $\langle p_t \rangle$ calculated by PACIAE+DCPC mode in the Pb-Pb collisions at $\sqrt{s_{NN}} = 2.76$ TeV, comparing with the Au-Au collisions at $\sqrt{s_{NN}} = 200$ GeV [27].

Particle type	d	\bar{d}	3He	${}^3\bar{He}$	$\frac{3}{\Lambda}H$	$\frac{3}{\Lambda}\bar{H}$
Pb-Pb(2.76 TeV)	1.00	1.05	1.16	1.24	1.17	1.22
Au-Au(200 GeV)	0.92	0.96	1.05	1.06	1.15	1.18

Furthermore, the results of light (anti)nuclei average transverse momentum $\langle p_t \rangle$ calculated by PACIAE+DCPC model in central rapidity Pb-Pb collisions at $\sqrt{s_{NN}} = 2.76$ TeV are given in Table III. As a comparison, the results [27] of light (anti)nuclei average transverse momentum $\langle p_t \rangle$ in Au-Au collisions at $\sqrt{s_{NN}} = 200$ GeV are also showed. Here we can see that the average transverse momentum of light anti-nuclei is slightly larger than that of the corresponding light nuclei. And the results of light (anti)nuclei average transverse momentum $\langle p_t \rangle$ in Pb-Pb collisions are larger than one of Au-Au collisions.

In Fig. 4 we show the integrated yields dN/dy of $d, \bar{d}, \frac{3}{\Lambda}H, \frac{3}{\Lambda}\bar{H}, {}^3He$ and ${}^3\bar{He}$ divided by N_{part} , as a function of N_{part} , respectively. All data points are normalized to the values obtained in the peripheral collisions

(50%-80%) with participant numbers 36. We choose the 50%-80% centrality bin as the reference of peripheral collisions because of the limited statistics of N_{part} and yield, as well as the strong fluctuation in the 80%-100% centrality bins. It shows that the yields of light (anti)nuclei and (anti)hyper-triton per participant nucleon increase rapidly with the increase of the number of participant N_{part} . Obviously, this distribution properties of light (anti)nuclei and (anti)hyper-triton production in Pb-Pb collisions at $\sqrt{s_{\text{NN}}} = 2.76$ TeV mainly depend on their mass number, i.e., the greater the mass number, the faster the yield increases.

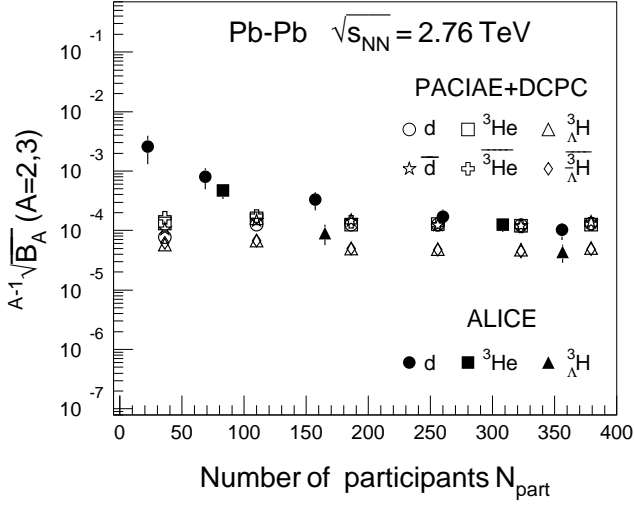


FIG. 5: Coalescence parameters B_A as a function of N_{part} for light (anti)nuclei in Pb-Pb collisions at $\sqrt{s_{\text{NN}}} = 2.76$ TeV. The open symbols represent our model results evaluated for different types of (anti)nuclei. The solid points are the data points from ALICE measurements evaluated with deuterons, hypertriton and ^3He [34, 36, 37, 39].

In heavy ion collisions, the coalescence process of light (anti)nuclei, and (anti)hypernuclei is historically described [15–17] by the coalescence parameter B_A . The differential invariant yield is related to the primordial yields of nucleons and is described by the equation:

$$E_A \frac{d^3 N_A}{d^3 P_A} = B_A (E_P \frac{d^3 N_P}{d^3 P_P})^A, \quad (6)$$

where $E d^3 N/d^3 p$ stands for the invariant yields of nucleons or light (anti)nuclei, and (anti)hypernuclei, and A are the atomic mass number, respectively. p_A, p_P denote their momentum, with $p_A = A p_P$ assumed. The phase-space information of $p(\bar{p})$ and $\Lambda(\bar{\Lambda})$, which is used as an input for the coalescence prescription, can be reproduced by the hydrodynamic blast-wave model.

The coalescence parameters B_A can be evaluated by comparing the invariant yields of the light (anti)nuclei and the primordial (anti)nucleons. Fig. 5 presents the

$A^{-1}\sqrt{B_A}$ as a function of N_{part} , which remain unchanged from central to peripheral collisions for our model results. B_2 and $\sqrt{B_3}$ calculated based on the invariant yields of $d, \bar{d}, ^3\text{He}(\bar{^3\text{He}}), ^3_\Lambda\text{H}(\bar{^3_\Lambda\text{H}})$ are consistent with the ALICE results [34, 36, 37, 39] as $N_{\text{part}} \geq 100$. In addition, we noticed that $\sqrt{B_3}$ of $^3_\Lambda\text{H}(\bar{^3_\Lambda\text{H}})$ is smaller than one of $^3\text{He}(\bar{^3\text{He}})$ even though the two nuclei have the same mass number. This reflects the strangeness content dependence of the coalescence parameter, i.e., there exists an additional penalty factor due to strangeness.

In a word, we hope utilizing the study of light (anti)nuclei and light (anti)hyper-triton, like their yields and ratios, their centrality dependence, their transverse momentum distributions, to seek a new clue to explore the new production mechanism for heavier antimatter in relativistic heavy ion collisions.

IV. CONCLUSION

In this paper, we use the PACIAE+DCPC model to investigate the properties of light (anti)nuclei and (anti)hyper-triton production in Pb-Pb collisions at $\sqrt{s_{\text{NN}}} = 2.76$ TeV with $|y| < 0.5$ acceptances. The integrated yields dN/dy of light (anti)nuclei $d(\bar{d})$, $^3\text{He}(\bar{^3\text{He}})$, as well as $^3_\Lambda\text{H}(\bar{^3_\Lambda\text{H}})$ are calculated by the DCPC model for each centrality bin. The results show that the yields of light (anti)nuclei and (anti)hyper-triton decrease rapidly with the increase of centrality bins. However, the yield ratios of light anti-nuclei to light nuclei and anti-hypertriton to hyper-triton are independent of centrality, which are irrelevant to the decreasing yields from central to peripheral collisions. In addition, the transverse momentum distributions of light anti(nuclei) are given in the 0-10% most central Pb-Pb collisions. With respect to light nuclei, the transverse momentum that the peak of distribution corresponded is nearly equal to the one of corresponding anti-nuclei. Our model results are in agreement with the ALICE experimental data. We also gained that the yields of light (anti)matter per participant nucleon increase linearly with the increase of the number of participants with N_{part} . Obviously, this distribution properties of light (anti)nuclei and (anti)hyper-triton production mainly depend on their mass number. At last we calculated and discussed coalescence parameters B_A of light (anti)nuclei and (anti)hypernuclei.

ACKNOWLEDGMENT

Finally, we acknowledge the financial support from NSFC(11475149, 11305144, 11303023). The authors thank Prof. Ben-Hao Sa, PH.D. Yu-Liang Yan for helpful discussions.

-
- [1] O. Chamberlain, E. Segrè, C. Wiegand *et al.*, Phys. Rev. **100**, 947(1955).
- [2] B. Cork, G. R. Lambertson, O. Piccioni *et al.*, Phys. Rev. **104**, 1193(1956).
- [3] T. Massam, T. Muller, B. Righini *et al.*, Nuovo Cim. **39**, 10(1965).
- [4] D. E. Dorfan, J. Eades, L. M. Lederman *et al.*, Phys. Rev. Lett. **14**, 1003(1965).
- [5] N. K. Vishnevsky *et al.*, Yad. Fiz. **20**, 694(1974).
- [6] Y. M. Antipov *et al.*, Yad. Fiz. **12**, 311(1970).
- [7] BRAHMS, PHENIX, PHOBOS, and STAR Collaboration. Nucl.Phys. A **757**, Issues 1–2, 1–283(2005).
- [8] H. Agakishiev *et al.* (STAR Collaboration), Nature **473**, 353(2011).
- [9] G. Baur, G. Boero, S. Brauksiepe *et al.*, Phys. Lett. B **368**, 251(1996).
- [10] G. B. Andresen, M. D. Ashkezari, M. Baquero-Ruiz *et al.*, Nature, **468**(7324), 673,(2010)
- [11] N. Sharma (ALICE Collaboration), J. Phys. G: Nucl. Part. Phys. **38**, 124189(2011).
- [12] B. I. Abelev *et al.*, (STAR Collaboration), Science **328**, 58(2010).
- [13] S. T. Butler and C. A. Pearson, Phys. Rev. **129**, 836(1963).
- [14] A. Schwarzschild and C. Zupancic, Phys. Rev. **129**, 854(1963).
- [15] H. H. Gutbrod, A. Sandoval, P. J. Johansen *et al.*, Phys. Rev. Lett. **37**, 667(1976).
- [16] J. Gosset, H. H. Gutbrod, W. G. Meyer *et al.*, Phys. Rev. C **16**, 629(1977).
- [17] M. C. Lemaire, S. Nagamiya, S. Schnetzer *et al.*, Phys. Lett. B **85**, 38(1979).
- [18] R. Mattiello, H. Sorge, H. Stöcker *et al.*, Phys. Rev. C **55**, 1443(1997).
- [19] L. W. Chen, C. M. Ko, Phys. Rev. C **73**, 044903(2006).
- [20] S. Zhang, J. H. Chen, H. Crawford *et al.*, Phys. Lett. B **684**, 224(2010).
- [21] V. Topor Pop and S. Das Gupta, Phys. Rev. C **81**, 054911(2010).
- [22] A. Andronic, P. Braun-Munzinger, J. Stachel *et al.*, Phys. Lett. B **697**, 203 (2011).
- [23] L. Xue, Y. G. Ma, J. H. Chen *et al.*, Phys. Rev. C **85**,064912 (2012).
- [24] J. Steinheimer, K. Gudima, A. Botvina *et al.*, Phys. Lett. B **714**, 85 (2012).
- [25] Y. L. Yan, G. Chen, X. M. Li *et al.*, Phys. Rev. C **85**, 024907(2012).
- [26] B. H. Sa, D. M. Zhou, Y. L. Yan *et al.*, Comput. Phys. Commun. **183**, 333(2012).
- [27] G. Chen, Y. L. Yan, D. S. Li *et al.*, Phys. Rev. C **86**, 054910(2012).
- [28] G. Chen, H. Chen, J. Wu *et al.*, Phys. Rev. C **88**, 034908(2013).
- [29] G. Chen, H. Chen, J. L. Wang *et al.*, J. Phys. G: Nucl. Part. Phys. **41**, 115102(2014).
- [30] J. L. Wang, D. K. Li, H. J. Li *et al.*, Int. J. Mod. Phys. E **23**, 1450088 (2014)
- [31] T. Sjöstrand, S. Mrenna, and P. Skands, J. High Energy Phys. **05**, 026(2006).
- [32] B. L. Combridge, J. Kripfgang, and J. Ranft, Phys. Lett. B **70**, 234(1977).
- [33] K. Stowe, An Introduction to Thermodynamics and Statistical Mechanics (Cambridge University, New York, 2007); R. Kubo, Statistical Mechanics (North-Holland, Amsterdam,1965).
- [34] B. Abelev (ALICE Collaboration), Phys. Rev. C **88**, 044910(2013).
- [35] M. Petran, J. Letessier, V. Petracek *et al.*, Phys. Rev. C **88**, 034907(2013).
- [36] J. Adam (ALICE Collaboration), arXiv:1506.08453v1 [nucl-ex],(2015).
- [37] J. Adam (ALICE Collaboration), arXiv:1506.08951v2 [nucl-ex],(2015).
- [38] R. Lea (ALICE Collaboration), Nucl. Phys. A **914**, 415(2013).
- [39] B. Abelev (ALICE Collaboration), Phys. Rev. C **88**, 044909(2013).